






ARTICLE

Once a reservoir, always a reservoir? Seasonality affects the pathogen maintenance potential of amphibian hosts

Mark Q. Wilber^{1,2}  | Michel E. B. Ohmer^{3,4,5} | Karie A. Altman^{4,6} |
 Laura A. Brannelly^{4,7}  | Brandon C. LaBumbard⁸ | Emily H. Le Sage⁹  |
 Nina B. McDonnell⁸ | Aura Y. Muñiz Torres⁸ | Caitlin L. Nordheim^{2,4} |
 Ferdinand Pfab² | Corinne L. Richards-Zawacki⁴  | Louise A. Rollins-Smith⁹ |
 Veronica Saenz⁴ | Jamie Voyles¹⁰  | Daniel P. Wetzel⁴ |
 Douglas C. Woodhams⁸ | Cheryl J. Briggs²

¹Department of Forestry, Wildlife, and Fisheries, University of Tennessee, Institute of Agriculture, Knoxville, Tennessee, USA

²Ecology, Evolution and Marine Biology, University of California, Santa Barbara, Santa Barbara, California, USA

³Living Earth Collaborative, Washington University in St. Louis, St. Louis, Missouri, USA

⁴Department of Biological Sciences, University of Pittsburgh, Pittsburgh, Pennsylvania, USA

⁵Department of Biology, University of Mississippi, Oxford, Mississippi, USA

⁶Department of Biology, St. Bonaventure University, St. Bonaventure, New York, USA

⁷Melbourne Veterinary School, Faculty of Veterinary and Agricultural Sciences, The University of Melbourne, Werribee, Victoria, Australia

⁸Department of Biology, University of Massachusetts Boston, Boston, Massachusetts, USA

⁹Department of Pathology Microbiology, and Immunology, Vanderbilt University School of Medicine, Nashville, Tennessee, USA

¹⁰Department of Biology, University of Nevada Reno, Reno, Nevada, USA

Correspondence

Mark Q. Wilber

Email: mwilber@utk.edu

Abstract

Host species that can independently maintain a pathogen in a host community and contribute to infection in other species are important targets for disease management. However, the potential of host species to maintain a pathogen is not fixed over time, and an important challenge is understanding how within- and across-season variability in host maintenance potential affects pathogen persistence over longer time scales relevant for disease management (e.g., years). Here, we sought to understand the causes and consequences of seasonal infection dynamics in leopard frogs (*Rana sphenoccephala* and *Rana pipiens*) infected with the fungal pathogen *Batrachochytrium dendrobatidis* (*Bd*). We addressed three questions broadly applicable to seasonal host-parasite systems. First, to what degree are observed seasonal patterns in infection driven by temperature-dependent infection processes compared to seasonal host demographic processes? Second, how does seasonal variation in maintenance potential affect long-term pathogen persistence in multi-host communities? Third, does high deterministic maintenance potential relate to the long-term stochastic persistence of pathogens in host populations with seasonal infection dynamics? To answer these questions, we used field data collected over 3 years on >1400 amphibians across four geographic locations, laboratory and mesocosm experiments, and a novel mathematical model. We found that the mechanisms that drive seasonal prevalence were different from those driving seasonal infection intensity. Seasonal variation in *Bd* prevalence was driven primarily by changes in host contact rates associated with breeding migrations to and from aquatic habitat. In contrast, seasonal changes in infection intensity were driven by temperature-induced changes in *Bd* growth rate. Using our model, we found that the maintenance potential of leopard frogs varied significantly throughout the year and that seasonal troughs in infection prevalence made it unlikely that leopard frogs were responsible for long-term

Funding information

U.S. Department of Defense, Grant/Award Number: RC-2638

Handling Editor: Chelsea L. Wood

Bd persistence in these seasonal amphibian communities, highlighting the importance of alternative pathogen reservoirs for *Bd* persistence. Our results have broad implications for management in seasonal host–pathogen systems, showing that seasonal changes in host and pathogen vital rates, rather than the depletion of susceptible hosts, can lead to troughs in pathogen prevalence and stochastic pathogen extirpation.

KEYWORDS

Batrachochytrium dendrobatidis, critical community size, disease dynamics, maintenance species, *Rana pipiens*, *Rana sphenocephala*, reservoir species, seasonal R_0 , seasonality

INTRODUCTION

From influenza in humans to anthrax in pastoral cattle to conjunctivitis in wild finches, seasonality is a critical driver of the timing and magnitude of disease outbreaks (Chikerema et al., 2012; Finkelman et al., 2007; Hosseini et al., 2004). Seasonality in host–pathogen systems is driven by periodic variation in host and pathogen vital rates and identifying the mechanisms underlying this variation is critical for predicting seasonal incidence (Altizer et al., 2006; Hirsch et al., 2016; Martinez, 2018). For example, a now famous case study by London and Yorke (1973) identified that seasonality in childhood diseases such as measles, chickenpox, and mumps was caused, in part, by increases in contact rates at the start of the school year. Similarly, in wildlife and livestock systems, seasonal changes in host contact rates associated with aggregation near limited resources (Brown et al., 2013; VanderWaal et al., 2017), seasonal birth pulses (Peel et al., 2014), and seasonal changes in immunity (Hosseini et al., 2004; Raffel et al., 2006) have been identified as mechanisms leading to seasonal fluctuations in infection prevalence. Despite substantial progress in a few well-studied human, livestock, and wildlife diseases, identifying the causes and consequences of seasonality for host–pathogen interactions remains a major challenge for disease management (Bozzuto & Canessa, 2019; Martinez, 2018).

Temperature drives seasonality in many host–pathogen systems by modulating the vital rates of hosts and pathogens (Altizer et al., 2006; Mordecai et al., 2017). Temperature can have particularly large effects on disease dynamics in ectotherms, such as amphibians, whose body temperatures can fluctuate throughout the year with concomitant effects on immune activity (Le Sage et al., 2021; Raffel et al., 2006). Chytridiomycosis, a disease caused by the aquatic fungal pathogen *Batrachochytrium dendrobatidis* (*Bd*) that is a major factor in declines of amphibian species worldwide (Kilpatrick

et al., 2010), is an emblematic example of temperature-dependent disease dynamics in ectotherms. Experiments have demonstrated that temperature directly affects within-host infection dynamics such as pathogen growth and host survival, but that the direction of the relationship is species dependent (Kilpatrick et al., 2010; Piotrowski et al., 2004; Raffel et al., 2013; Sonn et al., 2017). Similarly, while field studies have often demonstrated significant relationships between temperature and *Bd* infection prevalence and intensity (e.g., Barrile et al., 2021; Sonn et al., 2019; Woodhams & Alford, 2005), the direction and magnitude of the effect of temperature on *Bd* infection can be variable (Kilpatrick et al., 2010). In addition to absolute temperature, temperature variability and thermal mismatches between historic temperatures and current temperatures experienced by amphibian populations are predictive of changes in *Bd* prevalence, *Bd* infection intensity, and amphibian declines (Cohen et al., 2019; Greenspan et al., 2017; Raffel et al., 2013).

However, there remain three key knowledge gaps regarding the effects of temperature on population-level *Bd* dynamics, and seasonality in host–parasite interactions more generally. First, what are the relative contributions of temperature-dependent parasite and host infection processes compared to host demographic processes on seasonality in disease dynamics (e.g., Hirsch et al., 2016; Hosseini et al., 2004)? Because *Bd* infects amphibian hosts through an aquatic zoospore stage, temperature effects on *Bd* persistence in the environment can also drive seasonality in *Bd* dynamics. In fact, the mortality rate of *Bd* zoospores in the environment increases with increasing temperature (Woodhams et al., 2008), with the potential to drive seasonal variation in transmission. Moreover, breeding and recruitment are highly seasonal for many amphibian species (Cayuela et al., 2020). Seasonal changes in host density in aquatic environments due to breeding migrations and host demography could augment, offset, or dilute seasonal disease dynamics induced by within-host infection processes

that are temperature dependent (e.g., pathogen growth modulated by immune activity). By identifying the mechanisms driving seasonality, targeted seasonal management strategies can be developed to mitigate seasonal epizootics (Bozzuto & Canessa, 2019).

The second knowledge gap in seasonal host–parasite systems is, how does seasonality in host and pathogen vital rates drive variation in a species' ability to maintain a pathogen? And how does this temporal variation contribute to a species' ability to act as a maintenance species over time scales relevant for management (e.g., years)? Many wildlife pathogens, including *Bd*, infect multiple species (Clare et al., 2016). Particular species can independently maintain a pathogen in a community and act as a reservoir for the spread of the pathogen to other species (Viana et al., 2014). Despite the tendency to characterize the reservoir and maintenance potential of a host as an intrinsic attribute (Brannelly et al., 2018; Palmer, 2013; Viana et al., 2014), both ecological and seasonal context can affect this potential (Roberts & Heesterbeek, 2020). For example, temperature dependence in host and pathogen vital rates can mean that a maintenance species at one time of the year is no longer a maintenance species at another time. Dynamical disease models combined with seasonal infection data can quantify the seasonal maintenance potential of host species (Bozzuto & Canessa, 2019) but have rarely been applied to understand seasonal disease dynamics in multi-species host communities.

Demographic stochasticity, or random variation in survival and reproduction among hosts and pathogens, also plays a critical role in seasonal disease persistence (Bartlett, 1960; Haydon et al., 2002). However, assessing the maintenance potential of species often relies on model quantities derived in the assumed absence of demographic stochasticity (e.g., the fundamental reproductive number R_0 that is derived from deterministic host–pathogen models). The third knowledge gap in our understanding of seasonality in host–pathogen systems is, do hosts that are predicted to promote pathogen persistence in the absence of demographic stochasticity also enable long-term pathogen persistence in seasonal environments in the presence of demographic stochasticity? Host species that are predicted to robustly maintain a pathogen (e.g., have high seasonal R_0 , corresponding to pathogen invasion and long-term persistence; Rebelo et al., 2012; Bozzuto & Canessa, 2019), might in truth have a low probability of long-term pathogen maintenance given demographic stochasticity in host and pathogen dynamics. This could happen if a finite population of hosts is stochastically unlikely to maintain the pathogen through seasonal troughs in infection prevalence, despite a high potential for pathogen invasion. Concepts such as

critical community size, broadly defined as the population size above which long-term pathogen persistence is more likely (Viana et al., 2014), can capture this stochastic dimension of pathogen persistence. Given that seasonality is a pervasive component of many host–pathogen systems, quantifying the correspondence between deterministic and stochastic metrics of host maintenance potential has broad implications for effectively identifying maintenance species.

Here, we address these knowledge gaps by combining a novel modeling approach that accounts for within- and between-host infection processes with laboratory and mesocosm experiments and extensive field sampling of amphibian communities that are endemically infected with *Bd*. We focus our analysis on two widespread North American leopard frog species, *Rana pipiens* and *Rana sphenoccephala*. Leopard frogs provide an ideal species group to understand seasonality in host–pathogen systems because (1) they occur across a large geographical and climatological gradient in North America, allowing for robust conclusions to be drawn across varying seasonal and ecological contexts, (2) they are endemically infected with *Bd*, and (3) they exhibit seasonality in demographic (e.g., terrestrial-aquatic migrations) and immunological processes (Le Sage et al., 2021; Merrell, 1970). Thus, we hypothesized that both changes in host demographic processes and temperature-dependent changes in host susceptibility explain observed seasonal *Bd* dynamics. Using this amphibian–*Bd* system, we asked three questions broadly applicable to seasonality in host–pathogen systems. First, to what degree are observed seasonal patterns in infection driven by temperature-dependent infection processes (e.g., transmission and pathogen growth) compared to seasonal host demographic processes (e.g., reproduction and terrestrial-aquatic migrations)? Second, how does seasonal variation in maintenance potential affect long-term pathogen persistence in multi-host communities? Third, does high deterministic maintenance potential relate to the long-term stochastic persistence of pathogens in host populations with seasonal infection dynamics?

MATERIALS AND METHODS

System descriptions, field sampling, and experiments

We monitored seasonal *Bd* infection and prevalence dynamics in amphibian communities in four regions along a latitudinal gradient in eastern North America for 3 years (2017–2019) (see Figure 1a; Appendix S1; Table S1). Southern sites in Tennessee and Louisiana were sampled in all four seasons, while northern sites in

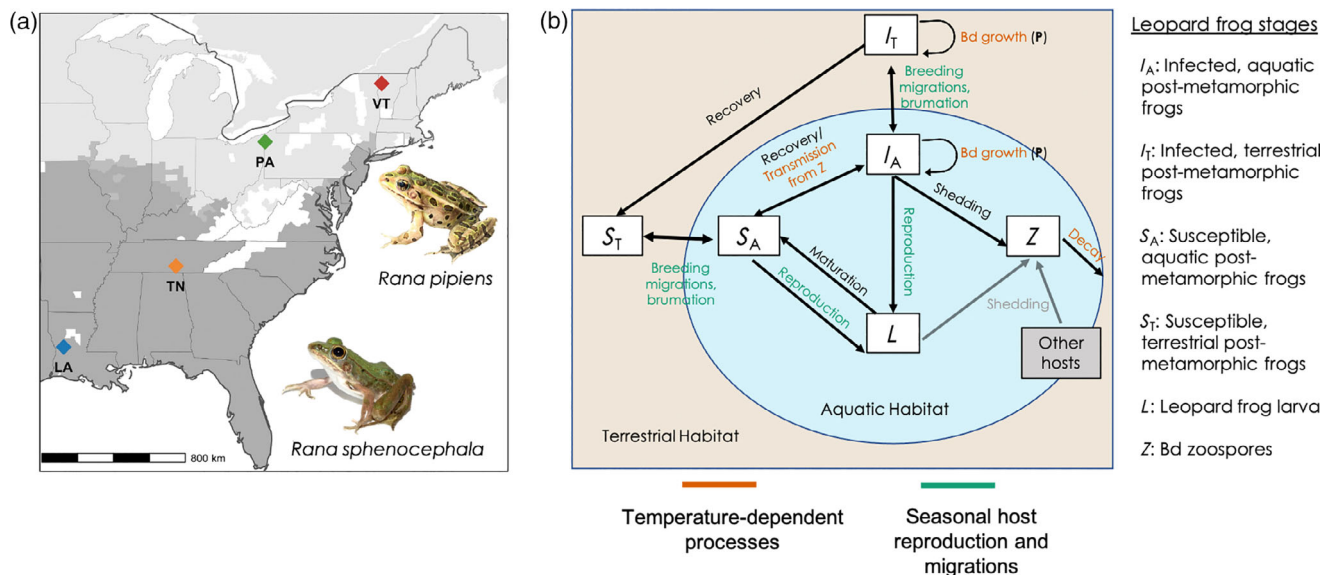


FIGURE 1 We combined (a) field, laboratory, and mesocosm data from four geographic locations and (b) a mathematical model to understand seasonal fungal infection dynamics of southern (*Rana sphenocephala*) and northern leopard frogs (*Rana pipiens*). Panel (b) provides a conceptual overview of the mathematical model given by Equation (2), which captures the seasonal movement, demography, and reproduction of leopard frogs as well as the infection dynamics of the fungus *Batrachochytrium dendrobatidis* (*Bd*). In (b), we distinguish between post-metamorphic leopard frogs that are in the terrestrial habitat (T) and those that are in the aquatic habitat (A). Those stages are implicitly defined in Equation (2). We assume that Larvae (L) and “other hosts” contribute to the pathogen pool through constant input of zoospores. The state variable P represents the *Bd* on an infected host and can change through within-host infection dynamics, such as *Bd* growth. Green represents host demographic processes that change seasonally and orange represents infection processes that are potentially temperature dependent.

Vermont and Pennsylvania were sampled in all seasons except winter. We surveyed at least five independent sites within each region, each site was typically surveyed three to four times during a given sampling season, for a total of 76,305 sampling events per region during the 3 years of the study (Appendix S1: Table S1). The target leopard frog species was the northern leopard frog (*R. pipiens*) in northern sites (Pennsylvania and Vermont), and the southern leopard frog (*R. sphenocephala*) in southern sites (Tennessee and Louisiana). The focal species were not found at all sites surveyed (Appendix S1: Table S1). At each site, we also collected surface water temperature every 30 min over 3 years using HOBO (Onset) data loggers.

We conducted visual encounter surveys after sunset, typically for at least 1 h. We collected all amphibians in individual plastic bags, changing gloves and rinsing nets in between individuals. For each animal, we measured snout–vent length and mass, and recorded life stage and sex (if known). We swabbed all animals to test for *Bd* by rubbing a fine-tipped rayon swab (Medical Wire #M113) five times across each of the dorsal and ventral surfaces, sides, and feet. *Bd* infection intensity was quantified with quantitative PCR following Hyatt et al. (2007), with a few modifications (Appendix S1). We released all amphibians

at the place of capture. Swabs were kept on ice while in the field and transferred to -20°C for storage. We swabbed a total of 1422 post-metamorphic leopard frogs across the four locations ($n = 382, 567, 411,$ and 62 in Louisiana, Tennessee, Pennsylvania, and Vermont, respectively).

We also performed a laboratory experiment with northern leopard frogs (*R. pipiens*) collected in Pennsylvania with the goal of comparing the growth of *Bd* infection on leopard frogs at different temperatures with natural infection loads. We used this experiment to inform and independently validate our inference on within-host *Bd* infection processes that we made using our dynamical model (described in *Model description*). The full laboratory experiment is described in Appendix S1. Finally, in mesocosms, we exposed *R. pipiens* larvae (i.e., tadpoles) to *Bd* to determine the potential of this life stage to maintain infection (described in Appendix S1).

Model description

We used host–parasite Integral Projection Models (IPM) to model the seasonal dynamics of *Bd* in leopard frogs

(Easterling et al., 2000; Metcalf et al., 2015; Wilber et al., 2016). IPMs are dynamic models for structured populations that link individuals, traits, and population dynamics (Ellner et al., 2016). Host–parasite IPMs are useful for modeling amphibian–*Bd* dynamics because they explicitly account for *Bd* infection intensity (i.e., load) and the distribution of *Bd* load in the host population, both of which are important drivers of disease dynamics in amphibian–*Bd* systems (Briggs et al., 2010). We used a reduced dimension host–parasite IPM where *Bd* load is modeled on the log scale. Reduced IPMs are low dimension approximations of full host–parasite IPMs and can facilitate the fitting of IPMs to population-level infection data (Wilber et al., 2021). The relationship between the full IPM and reduced IPM is described in Appendix S2.

The reduced IPM is a discrete-time model that tracks changes in five state variables describing leopard frog and *Bd* population dynamics: the density of leopard frog larvae (i.e., tadpoles, L), density of susceptible post-metamorphic leopard frogs (S), density of infected post-metamorphic leopard frogs (I), the total amount of log(*Bd* parasites) on infected post-metamorphic leopard frogs (P), and the density of *Bd* zoospores in the water (Z). The time step of our model is 7 days, which is on the scale of a generation time of *Bd* (between 4 and 10 days depending on temperature; Piotrowski et al., 2004; Woodhams et al., 2008). The total density of post-metamorphic leopard frogs at time t is $N(t) = S(t) + I(t)$ (per m^3). “Post-metamorphic” refers to adults and juveniles (i.e., post-metamorphic individuals not yet reaching sexual maturity), which we modeled as a single life stage. This was a statistical rather than biological decision, as the ratio of adults to juveniles swabbed varied by location and through time, such that it was difficult to statistically separate the effects of season and life stage on infection prevalence and intensity.

The dynamics for leopard frog larvae L are

$$L(t+1) = r' \frac{N(t)}{2} \mathbf{1}_{t=t_{\text{repro}}} + L(t) s_L (1 - m_L) \quad (1)$$

where r' is the number of larvae produced by a female and $N(t)/2$ gives the number of females assuming a 50:50 sex ratio. The term $\mathbf{1}_{t=t_{\text{repro}}}$ is an indicator variable that is one when the current time t is equal to the time within a year t_{repro} that is midway between when leopard frog breeding typically begins and ends at a location and zero otherwise. Thus, we assume that reproduction happens once per year. Note that breeding can happen twice per year (once in the spring and once in the fall) in populations of southern leopard frogs (*R. sphenoccephala*), such as those in Louisiana and Tennessee in our study. Because we observed that fall breeding happened less consistently than spring breeding, we only considered spring breeding in our models.

The parameter m_L is the probability of larvae metamorphosing in a time step and s_L gives the survival probability of amphibian larvae over a time step. Larval amphibians recruit into the susceptible post-metamorphic class with a density-dependent probability $e^{-KN(t)}$ (see [9] in Equation 2; Briggs et al., 2005), where K gives the strength of density dependence. While amphibian larvae can be infected with *Bd*, we did not explicitly model infection dynamics in larvae because we were rarely able to sample leopard frog larvae (45 larvae sampled over 3 years across all locations) and did not detect *Bd* on any of the sampled larvae. From our mesocosm experiment (Appendix S1), we also determined that larval *R. pipiens* resist infection from *Bd*.

The dynamics of *Bd* infection on post-metamorphic amphibians and for zoospores in the zoospore pool are given by (Figure 1b)

$$\begin{aligned}
 S(t+1) &= L(t) \underbrace{s_L m_L e^{-KN(t)}}_{(9)} + S(t) s_0 e^{-\beta Z(t) \mathbf{1}_{\text{in water at } t}} + s_0 s_I l_I(\alpha_t) I(t) \\
 I(t+1) &= S(t) s_0 \underbrace{\left[1 - e^{-\beta Z(t) \mathbf{1}_{\text{in water at } t}} \right]}_{(1)} + s_0 s_I \underbrace{\left(1 - l_I(\alpha_t) \right)}_{(2)} I(t) \\
 P(t+1) &= S(t) s_0 \underbrace{\left[1 - e^{-\beta Z(t) \mathbf{1}_{\text{in water at } t}} \right]}_{(3)} \underbrace{a}_{(4)} + I(t) s_0 \underbrace{s_I}_{(4)} \underbrace{\left[a(1 - l_I(\alpha_t)) + b \zeta \phi(\alpha_t) \right]}_{(5)} + P(t) b s_0 s_I \underbrace{\left[1 - l_I(\alpha_t) \right]}_{(5)} \\
 Z(t+1) &= \underbrace{I(t) \lambda e^{\frac{P(t)}{T}} e^{\frac{\sigma_F^2}{2}}}_{(6)} \mathbf{1}_{\text{in water at } t} + \underbrace{s_Z}_{(7)} Z(t) + \underbrace{\omega}_{(8)}.
 \end{aligned} \quad (2)$$

All parameters are defined in Table 1. The dynamics of the state variables in Equation (2) are affected by nine processes: transmission (1), loss of infection (2), *Bd* load upon initial infection (3), survival given infection (4), growth of infection (5), pathogen shedding (6), zoospore survival (7), external contributions to the zoospore pool (8), and larvae recruitment (9) (described at the start of *Model description*).

First, consistent with the life history of the leopard frog species in this study, we assumed that post-

metamorphic leopard frogs are in water and thus in contact with infective *Bd* zoospores during the breeding season and, for northern leopard frogs in Pennsylvania and Vermont, when brumating during the winter (Cunjak, 1986). Otherwise, we assumed that post-metamorphic leopard frogs are in the terrestrial environment with limited contact with the main body of water resulting in transmission rate ($\beta' = \beta/7$ days) equal to zero (Figure 1b). The transmission parameter β' is an aggregate parameter that describes both contact rate and the

TABLE 1 Parameters used in the reduced IPM.

Parameter	Description	Source
s_0	Uninfected survival probability over 7 days	Literature (AmphibiaWeb, 2021)
s_I	Load-independent reduction in survival probability of infected host relative to an infected host	Fit models with $s_I = 1$ and subsequently explored values between 0.97 and 1
m_L	$(1/m_L) \times \Delta t$ gives the average length of the tadpole stage in days	Literature (AmphibiaWeb, 2021)
s_L	Larvae survival probability over 7 days	Literature (Appendix S1: Tables S2 and S3)
a	Change in $\log(Bd$ load) when $\log(Bd$ load) is 0 (i.e., $\log(Bd$ growth rate))	Estimated from field data
a_1	The effect of mean temperature in the previous week on a	Estimated from field data and lab experiment
b	Slope of the <i>Bd</i> growth function on the log scale	Estimated from lab experiment
σ_F^2 (σ_F)	Variance (standard deviation) in the population-level $\log(Bd$ load) distribution	Estimated from field data
l_I	Loss of infection probability in a 7-day time step, independent of <i>Bd</i> load.	Estimated from field data
μ_l	$\log(Bd$ load) when loss of infection probability is 0.5	Estimated from field data
σ_l	Shape parameter specifying how loss of infection probability changes with $\log(Bd$ load).	Fixed at 1.15 (Appendix S2)
β'	Transmission parameter (m^3 per day) $\beta = \beta' \times 7$ days	Estimated from field data
β_1	The effect of temperature on β'	Estimated from field data
λ	Average zoospores shed per unit of pathogen on the host	Literature (Reeder et al., 2012).
ω	External contribution of zoospores per time step per m^3	Estimated from field data
$s_Z(T)$	Temperature-dependent zoospore survival probability in a 7-day time step	Literature (Woodhams et al., 2008)
K	Density dependence in tadpole recruitment (m^3)	Explored values of e^4 , e^8 , and e^{10} that yielded a realistic range of post-metamorphic densities
r'	Number of tadpoles produced per post-metamorphic female frog at yearly reproduction	Literature (AmphibiaWeb, 2021)
$1_{\text{in water at } t}$	Indicator variable that is 1 during brumation and breeding	Literature and personal field observations (AmphibiaWeb, 2021)
$1_{t=t_{\text{repro}}}$	Indicator variable that is one when a host reproduction occurs at time t_{repro} each year	Literature and personal field observations (AmphibiaWeb, 2021)

Note: A time step in the IPM is 7 days. Parameters with a boldface **Estimated** are those that we statistically inferred by fitting our reduced IPM to field data or by fitting IPM vital rate functions to data from our laboratory experiment (Appendix S1). Values and uncertainty in estimated parameters are given in Appendix S1: Tables S2 and S3.

Abbreviations: *Bd*, *Batrachochytrium dendrobatidis*; IPM, Integral Projection Models.

probability of infection given contact. We refer to the probability of infection given contact as susceptibility henceforth.

Second, we allowed the probability of losing infection in a time step $l_t(\alpha_t)$ to depend on the current infection load of an amphibian, with increasing load decreasing the probability of losing infection (Appendix S1: Figure S1). The parameter α_t scales the loss of infection probability based on the mean log(pathogen load) at time t (Appendix S2). Third, we let the mean log(pathogen load) obtained upon initial infection take the value a , which is defined as the log(pathogen load) at the end of a time step following infection by one *Bd* zoospore (i.e., log(pathogen growth rate)).

Fourth, consistent with our experimental data (Appendix S1: Figure S1), we assumed that post-metamorphic leopard frog survival over a time step given *Bd* infection s_0s_t is independent of pathogen load for the range of loads we observed in our study (0 to $10^{7.8}$ copies of *Bd* DNA per swab). Fifth, again consistent with our experimental observations (Appendix S1: Figure S1), we assumed that the average change in log(*Bd* load x_t) on a host over a 7-day time period, conditional on infection, was described by $x_{t+1} = a + bx_t$. The parameter a is the log(pathogen growth rate) and the parameter b captures density dependence in pathogen growth (where $b \leq 1$). The terms ζ and $\phi(\alpha_t)$ in Equation 2 quantify how load-dependent loss of infection interacts with pathogen growth (Appendix S2). Sixth, based on previously published results (DiRenzo et al., 2014; Reeder et al., 2012), we assumed that *Bd* shedding rate is directly proportional to *Bd* load on leopard frogs. Consistent with our assumption

about transmission, we assume that shedding only contributes to the zoospore pool when post-metamorphic frogs are in the water. Seventh, zoospores survive in the environment with a per time step probability of s_Z .

Eighth, we assumed that there is an external contribution of zoospores ω to the zoospore pool per time step (Figure 1b). In the four locations we consider here, there are between 12 and 22 amphibian species, many of which can be infected with *Bd* at various times throughout the year. Rather than trying to model the contributions of each of these species, we assumed that their contribution to *Bd* dynamics on post-metamorphic leopard frogs came primarily through their contributions to the zoospore pool Z .

Question 1: To what degree are observed seasonal patterns in infection driven by temperature-dependent infection processes compared to seasonal host migrations and reproduction?

We sought to disentangle the relative contribution of seasonality in host demography (e.g., seasonal reproduction and terrestrial-aquatic migrations) and temperature-mediated seasonality in host and pathogen vital rates (e.g., pathogen survival or host immunity) on seasonal patterns of *Bd* infection. To this end, we compared four different dynamic models, using temperature data directly observed in the field (Table 2; Appendix S1: Figure S2). To answer this question, we used statistical inference where we (1) defined candidate reduced IPMs,

TABLE 2 Summary of the seasonal processes included in the four different reduced IPM models fit to the field data.

Model name	Susceptibility varies with temperature	<i>Bd</i> growth varies with temperature	Zoospore decay varies with temperature	Host reproduction is seasonal	Host migrations are seasonal
Baseline ($l_t, \sigma_F, a, \beta', \omega$)	–	–	X	X	X
Baseline + temperature-dependent susceptibility ($l_t, \sigma_F, a, \beta', \beta_1, \omega$)	X	–	X	X	X
Baseline + temperature-dependent <i>Bd</i> growth ($\mu_t, \sigma_F, a, a_1, \beta', \omega$)	–	X	X	X	X
Baseline + temperature-dependent <i>Bd</i> growth and susceptibility ($\mu_t, \sigma_F, a, a_1, \beta', \beta_1, \omega$)	X	X	X	X	X

Note: An X indicates that the seasonal process was included in the model and a – indicates that the process was not included. The parameters in the parentheses are those that were statistically estimated when fitting the given model to the field data (Table 1; Appendix S3). Abbreviations: *Bd*, *Batrachochytrium dendrobatidis*; IPM, Integral Projection Models.

(2) fit these models to our observed field data (see *Model fitting*), (3) statistically compared models, and (4) made inference on estimated parameters.

Our first model (Baseline) hypothesized that seasonal patterns in *Bd* infection dynamics on leopard frogs were driven exclusively by temperature-dependent zoospore survival and seasonality in host terrestrial-aquatic migrations and reproduction. Woodhams et al. (2008) previously quantified a decreasing, nonlinear relationship between zoospore survival (s_z) and temperature and we used that relationship throughout this study. For the Baseline model, neither on-host *Bd* growth rate (a) nor the susceptibility component of transmission varied with temperature. However, the contact component of transmission β' varied seasonally when post-metamorphic leopard frogs left and returned to the aquatic environment (Cunjak, 1986). We inferred five parameters of the Baseline model by fitting it to the observed *Bd* prevalence and intensity trajectories from the field data at each location (namely, l_b , σ_F , a , β' , and ω ; Table 1). All other parameter values were obtained from the literature or our lab experiments (Table 1).

In the second model (Baseline + temperature-dependent susceptibility), we hypothesized that host susceptibility to infection (i.e., probability of infection given contact) could also vary with temperature (Table 2; Le Sage et al., 2021). Specifically, we modeled temperature-dependence in host susceptibility as $\beta'(T) = \beta' \exp(\beta_1 T)$, where β_1 is the effect of temperature on the host susceptibility component of β' and T is the average observed air temperature over the previous week, which closely matches observed water temperature (Appendix S1: Figure S2). The Baseline + temperature-dependent susceptibility model still included temperature-dependent zoospore survival and seasonal changes in the contact component of β' due to terrestrial-aquatic migrations. We inferred six parameters of the Baseline + temperature-dependent susceptibility model by fitting it to the field data (namely, l_b , σ_F , a , β' , β_1 , and ω ; Table 1).

The third model (Baseline + temperature-dependent *Bd* growth), included temperature-dependent zoospore survival and seasonal changes in the contact component of β' due to host movements, but also hypothesized that temperature affected *Bd* growth rates (Table 2). We modeled temperature-dependent $\log(\textit{Bd}$ growth rate a) as $a(T) = a + a_1 T$, where T was the average temperature over the previous week and a_1 was the effect of temperature on *Bd* growth rate. We inferred six parameters of the Baseline + temperature-dependent *Bd* growth model by fitting it to the field data (namely, μ_b , σ_F , a , a_1 , β' , and ω ; Table 1).

Finally, the fourth model (Baseline + temperature-dependent *Bd* growth and susceptibility) included

an effect of temperature on both *Bd* growth and the susceptibility component of β' (Table 2). We inferred seven parameters by fitting this model to the field data (namely, μ_b , σ_F , a , a_1 , β' , β_1 , and ω ; Table 1).

Model fitting

We statistically fit each model to the field data at the four locations, relying on information from the literature and our experiments to aid in parameterization (Table 1, see Appendix S3 for details). In Table 1, we identify which parameters we statistically infer using the field data and which we extracted from previous estimates in the literature or from our lab experiments. The field data that we used to fit the model were the observed trajectories of *Bd* prevalence and *Bd* infection intensity. We used inverse estimation to fit our four reduced IPM models to the observed field data (González et al., 2016). Inverse estimation is a form of trajectory matching where we (1) chose a set of initial values for the parameters we are estimating for a particular model (given in Table 2, parameters we were not estimating were fixed at their preassigned values given in Appendix S1: Tables S2 and S3), (2) simulated our reduced IPM model through time with the chosen parameter values, (3) compared the predicted trajectories from the reduced IPM of *Bd* prevalence and intensity to the observed *Bd* prevalence and intensity data, (4) updated our parameter values such that we improved the fit (e.g., maximized the likelihood) between the reduced IPM predictions and our observed data, and (5) repeated until we converged on the optimal parameter values (or a posterior distribution of parameter values given we used a Bayesian model fitting approach; Appendix S3). Note that we did not have capture–recapture data in this study. Instead we are making inference from observed trajectories of population-level prevalence and infection intensity.

A key unknown when parameterizing the model was the density of post-metamorphic amphibians. Disentangling true host density and observed host density is challenging without capture–mark–recapture data, which we did not have. Therefore, we instead fit our models under three different assumptions regarding the density of post-metamorphic leopard frogs that spanned the possible range of densities at our locations: high (0.14 hosts per m^3), medium (0.002 hosts per m^3), and low (0.0003 per m^3). These densities refer to maximum seasonal densities in the aquatic habitat that occur during breeding. We set these densities by varying the density-dependent recruitment parameter K in our model (Table 1). We also did not quantify the seasonal density of larvae $L(t)$ or the density of zoospores in the water $Z(t)$ in our field studies.

However, once we specified K , these state variables were predicted by our parameterized model (see Equation 2). If observations of $L(t)$ and $Z(t)$ were available, these estimates could be used to directly estimate parameters that we fixed based on previous studies (e.g., s_Z , Table 1).

For each location, we examined a total of 12 fitted models (4 seasonal hypotheses \times 3 density assumptions). We compared the fitted models using deviance information criteria (DIC) (Gelman et al., 2014), where lower DIC values indicated superior out-of-sample performance. We also ensured that our fitted models captured dominant seasonal patterns in the data by (1) calculating the percent of sampling dates where >4 post-metamorphic frog were sampled and our observed prevalence was not significantly different than predicted prevalence (using binomial tests with a Bonferroni correction for multiple comparisons), (2) calculating the R^2 value between observed and predicted Bd infection intensity for the best-fit model for each location (where “best” was determined by the lowest DIC), and (3) visually comparing predicted trajectories with the observed field observations.

Question 2: How does seasonal variation in host maintenance potential affect the long-term persistence of a pathogen?

We performed analytical and simulation-based analyses of our best predictive models using the parameters and parameter uncertainty statistically inferred in Question 1. We analyze the predictions from our “best” models (i.e., lowest DIC) regarding how seasonal variation in leopard frog maintenance potential affected long-term Bd persistence (e.g., persistence for many years). The parameters that we statistically inferred for each model are given in Table 2 and their values and uncertainty are provided in Appendix S1: Tables S2 and S3. The values of parameters that were fixed based on previous estimates in the literature (i.e., that we did not try to statistically infer in Question 1) are also provided in Appendix S1: Tables S2 and S3. Given the relatively small sample size of northern leopard frogs ($n = 62$) and the large uncertainty around the fitted model parameters in Vermont (Appendix S1: Tables S2 and S3), we only considered Louisiana, Tennessee, and Pennsylvania leopard frog populations for this portion of the analysis.

To address question 2, we first approximated the observed seasonal water temperature T at a given location with a sinusoidal curve where maximum and minimum temperatures were equal to the maximum and minimum temperatures observed at each location (Appendix S1: Figure S2): $T = ((T_{\max} - T_{\min})/2)(1 - \cos(2\pi\tau/364)) + T_{\min}$, where τ is the day within the

year. We used 364 days such that 1 year represented 52 weekly time steps. The minimum and maximum temperatures we used for each location were based on our empirical temperature data at each location (Appendix S1: Figure S2) and were as follows: Louisiana 4–30°C, Tennessee 4–27°C, and Pennsylvania 4–25°C. We approximated observed water temperatures with this sinusoidal curve to ask, if temperature followed a repeatable seasonal pattern approximately consistent with what has been observed, could Bd persist for many years on leopard frogs alone? A sinusoidal approximation allowed us to extrapolate repeatable seasonal temperature fluctuations arbitrarily far forward in time (Appendix S1: Figure S2). The sinusoidal temperature equation assumes that minimum seasonal water temperature occurs on 1 January, which is generally consistent with our observations (Appendix S1: Figure S2).

We calculated three metrics from our best-fit seasonal models. First, we calculated instantaneous R_0 from our reduced IPM. Instantaneous R_0 describes the ability of Bd to invade an uninfected leopard frog population at a specific moment in time, given the current host density and temperature-dependent infection parameters. It is defined as the average number of infected hosts produced by an average infected host in a fully susceptible population if the current conditions were held constant. Instantaneous R_0 can be used to define the maintenance potential of a host at a specific moment in time (Palmer, 2013). When instantaneous R_0 is highest over the course of the year, then the instantaneous invasion probability of Bd into the leopard frog population is highest. Instantaneous R_0 based on Equation (2) is

$$R_0(t, T) = \left(\frac{N(t)s_0\beta'(T)}{1 - s_Z(T)} \right) \left(\frac{\lambda e^{M^*(T)} e^{\sigma_T^2/2}}{1 - s_0s_I[1 - l_I(M^*(T))]} \right) \quad (3)$$

where $M^*(T)$ gives the expected Bd load on an infected host at temperature T (Wilber et al., 2021). All other parameters are defined above and in Table 1. Equation (3) shows that instantaneous R_0 varies as a function of temperature (e.g., $s_Z(T)$ indicates zoospore survival varies with temperature) and as a function of time, independent of temperature (e.g., $N(t)$, where $N(t)$ is the density of post-metamorphic leopard frogs at time t in the year).

Instantaneous R_0 changes over time and the value at any specific time does not reflect the ability of a pathogen to invade and persist in a host population over longer periods, such as a year. Therefore, we “integrated” over these instantaneous R_0 values to calculate a seasonal R_0 value that can be interpreted as the asymptotic ratio of epidemiological “births” over two successive generations (Appendix S4, Bacaër & Ait Dads, 2012). When seasonal

$R_0 > 1$, *Bd* introduced at any time in the year will deterministically invade and persist in the population over multiple seasons, even if instantaneous $R_0 < 1$ at the time of invasion (Bacaër & Ait Dads, 2012). Conceptually, instantaneous $R_0 < 1$ at the moment of pathogen invasion indicates that pathogen prevalence will initially start to decline, but seasonal $R_0 > 1$ tells us that, at some point during the year, instantaneous $R_0 > 1$ such that pathogen prevalence will increase. Overall, when seasonal $R_0 > 1$, the pathogen will grow more than it declines over the course of a year, leading to deterministic pathogen invasion and persistence over multiple years (Bacaër & Ait Dads, 2012; Rebelo et al., 2012). Thus, seasonal R_0 provides a metric for long-term deterministic maintenance potential. We incorporated uncertainty into our predictions of instantaneous and seasonal R_0 by propagating the estimated uncertainty in parameters inferred in Question 1 through to the values of R_0 .

Question 3: Does high seasonal maintenance potential predict long-term stochastic pathogen persistence?

For our deterministic models, seasonal $R_0 > 1$ means that post-metamorphic leopard frogs can maintain *Bd* independent of any other amphibian species. However, stochasticity can make long-term persistence of a pathogen in a host population unlikely (Almberg et al., 2010), even when seasonal $R_0 > 1$. To test whether seasonal $R_0 > 1$ corresponded to increased stochastic persistence of *Bd* in post-metamorphic leopard frog populations, we calculated the critical community size (CCS) for leopard frogs using the best model and its statistically inferred parameters as identified in Question 1 (Appendix S1: Tables S2 and S3). We defined the CCS as the number of post-metamorphic leopard frogs (density \times area) needed in a population such that the probability of pathogen persistence over 10 years was $\geq 50\%$ (Almberg et al., 2010). We tested the prediction that increased seasonal R_0 corresponded to a decreased CCS.

To calculate the CCS, we included demographic stochasticity in both leopard frog and *Bd* population dynamics. We recast our best-fit reduced IPMs as equivalent full IPMs that can accommodate demographic stochasticity in host populations and zoospore populations in the environment (Appendix S2). We used the median parameter estimates from the best reduced IPMs inferred in Question 1 under a high-density assumption (0.14 post-metamorphic individuals per m^3). We performed our CCS analyses using these median estimates as they predicted deterministic, long-term persistence of *Bd* in Louisiana, Pennsylvania, and Tennessee (see *Results*). We

stochastically simulated the full IPM for 10 years under different assumptions of host population size. We used host abundances from 14 to 140, which corresponded to aquatic habitat areas from 100 to 1000 m^3 under a high-density assumption. For each abundance level, we simulated the stochastic model 500 times and recorded whether or not *Bd* persisted in the host community for 10 years. The initial conditions of the stochastic model were set to match the equilibrium conditions from a deterministic version of the model.

When calculating instantaneous R_0 , seasonal R_0 , and CCS, we removed any external contribution from the zoospore pool when calculating the metrics. We did this to isolate the contribution of post-metamorphic leopard frogs to *Bd* persistence.

RESULTS

Question 1: To what degree are observed seasonal patterns in infection driven by temperature-dependent infection processes compared to seasonal host migrations and reproduction?

Host demographic processes associated with changes in contact with the zoospore pool, such as leaving and returning to aquatic habitats during breeding and brumation, largely accounted for changes in *Bd* prevalence over the course of a season. In other words, once we accounted for how temperature affected *Bd* load dynamics, we generally did not need to invoke any additional temperature dependence in the susceptibility component of transmission (i.e., probability of infection given contact) to describe the seasonal changes in *Bd* prevalence (DIC values were equivalent or lower for Baseline + temperature-dependent *Bd* growth compared to Baseline + temperature-dependent *Bd* growth and susceptibility for Tennessee, Pennsylvania, and Vermont populations; Appendix S1: Figure S3; Figure 2). For these three locations, models without any effects of temperature on host susceptibility to gaining infection predicted that, consistent with the observed data, *Bd* prevalence declined to low values when post-metamorphic leopard frogs spent less time in the water following breeding and thus experienced reduced transmission as they were not contacting the zoospore pool. The models predicted that prevalence rapidly returned to high levels when frogs returned to the aquatic environment at the onset of the breeding season (Figure 2).

Populations from Louisiana were an exception (Appendix S1: Figure S3). Here, our model predicted that a significant negative effect of temperature on the susceptibility component of transmission improved model predictions, even after accounting for temperature

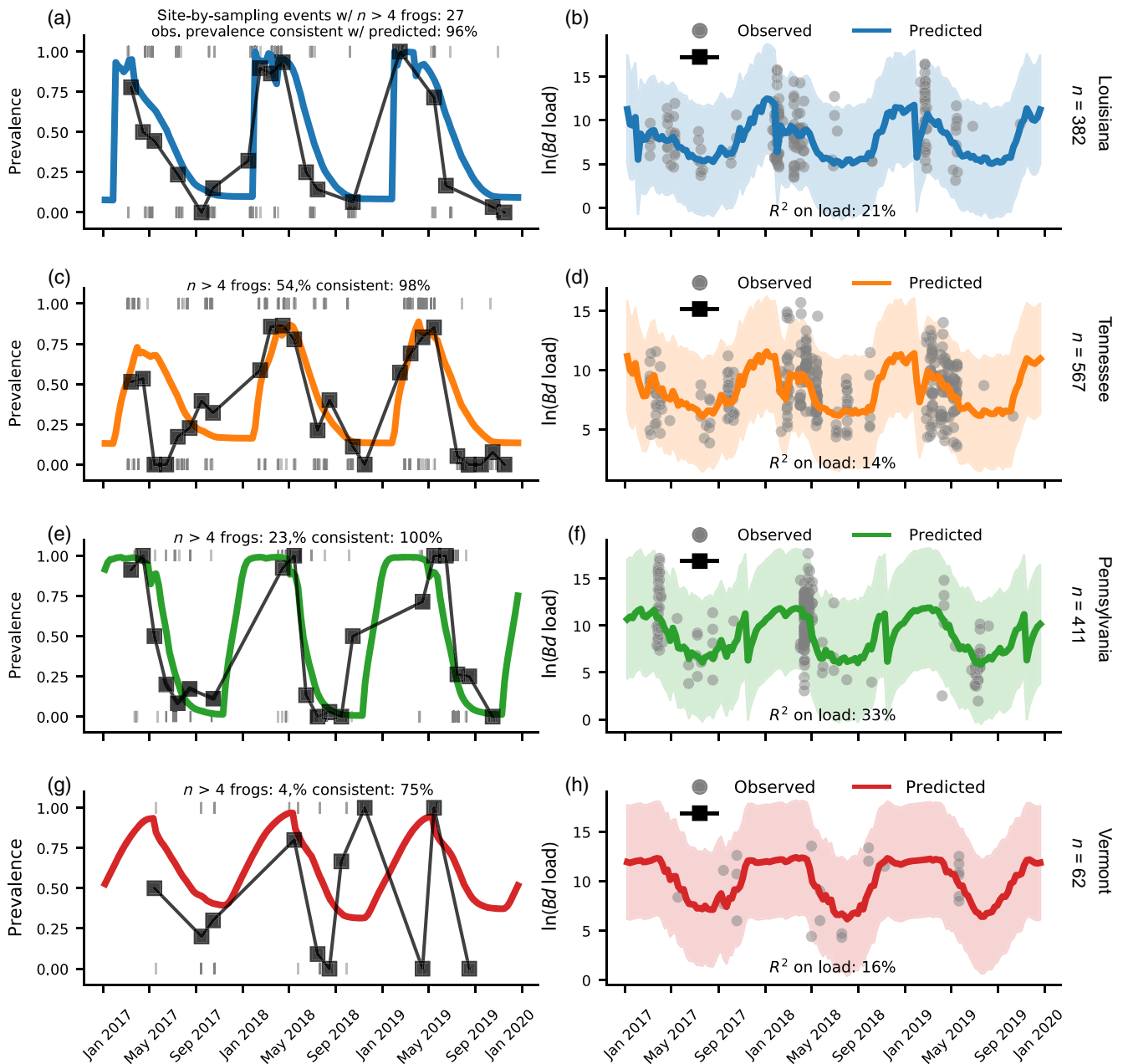


FIGURE 2 Best-fit model predictions and observed *Batrachochytrium dendrobatidis* (*Bd*) prevalence and load data on southern and northern leopard frogs. Each row gives the observed and predicted infection trajectories from a location. The number of post-metamorphic leopard frogs sampled for *Bd* at each location is given under each location name. The colored lines give the predictions from the model with the lowest deviance information criteria for each location under an assumption of low host density (0.0003 per m³). The shaded region gives the 95% prediction interval of ln *Bd* load from the best model. For (a, c, e, g), gray lines indicate whether or not a sampled host was positive (1) or negative (0) for *Bd* when sampled. Black points and lines give the mean observed monthly *Bd* prevalence on leopard frogs, pooled across all sites sampled within a location. For (b, d, f, h), gray points give the observed ln *Bd* load for sampled leopard frogs that were *Bd* positive. Goodness of fit is indicated by percent of site-by-sampling events where observed *Bd* prevalence was not significantly different than predicted prevalence and the R^2 for infection load predictions.

dependence in *Bd* load dynamics (the model with the lowest DIC was the Baseline + temperature-dependent *Bd* growth and susceptibility model, Appendix S1: Figure S3). This result was driven by data from

January–March 2017. Seasonally high air and water temperatures across these 3 months (average temperature of 16°C compared to a 20-year average air temperature of 12°C across these 3 months) correlated with a

reduction in *Bd* prevalence across Louisiana sites (Figure 2), resulting in a predicted negative effect of temperature on susceptibility.

Across all locations, our best-fit models predicted a negative effect of temperature on *Bd* growth rate, such that $\log(\text{Bd load})$ on post-metamorphic leopard frogs was predicted to be lowest during the warmest months (June, July, August) and highest during the coldest months (December, January, February; Figure 2). This result was qualitatively consistent with our laboratory experiment (Appendix S1: Figure S4).

Question 2: How does seasonal variation in host maintenance potential affect the long-term persistence of a pathogen?

Our best-fit models predicted that, for all locations, instantaneous R_0 (our metric of host maintenance potential) was highest in the coolest months when leopard frogs were present in the aquatic habitat (Figure 3a–c). This was when mean $\log(\text{Bd load})$ and prevalence were greatest (Figure 2).

Our analysis of seasonal R_0 predicted that post-metamorphic leopard frogs could maintain *Bd* in the population at the highest host densities we explored and when *Bd*-induced host mortality was 0 ($s_I = 1$; Figure 3g–l). However, when we assumed *Bd*-induced mortality was minimal, but present (e.g., $s_I = 0.97$, corresponding to a post-metamorphic host surviving on average 233 days with infection, Appendix S1: Figure S1c), it was unlikely that southern leopard frogs in Tennessee or northern leopard frogs in Pennsylvania could maintain *Bd* in the population for any density we explored. All median seasonal R_0 values were <1 and deterministic simulations of models using median parameter estimates and no external zoospore pool led to eventual *Bd* extinction (Figure 3g–l). For southern leopard frogs in Louisiana, we were unable to provide a biologically meaningful estimate of seasonal R_0 for the best-fit model Baseline + temperature-dependent *Bd* growth and susceptibility (see Appendix S3). However, relevant for our subsequent analyses, deterministic simulations of the Louisiana model predicted long-term *Bd* persistence (Figure 3d–f).

Question 3: Does high seasonal maintenance potential predict long-term stochastic pathogen persistence?

When we included demographic stochasticity in frog and zoospore dynamics, we found that seasonal R_0 did not correspond with long-term persistence of *Bd* (Figure 4). Despite leopard frogs in Tennessee and Pennsylvania

having similar values of seasonal R_0 under a high-density assumption (median values of 1.9 and 1.35, respectively), these locations had drastically different critical community sizes (CCS). In Tennessee, our high-density model predicted that leopard frogs had a 50% probability of maintaining *Bd* for >10 years when host abundance was 100 in an area of 714 m^3 (Figure 4). For reference, we typically observed no more than 17 post-metamorphic leopard frogs in an area of $10,000 \text{ m}^3$ in Tennessee (though this was likely an underestimate of true abundance). In Pennsylvania, leopard frogs alone could not maintain *Bd* for >10 years for any of the population sizes that we tested (Figure 4).

In Louisiana, our models predicted a lower CCS: at least 51 frogs in an area of 365 m^3 were needed for a 50% probability of 10 or more years of *Bd* persistence (Figure 4). We typically observed no more than 28 frogs in an area of approximately $11,000 \text{ m}^3$ in Louisiana. These results were qualitatively unchanged when we stochastically simulated our best-fit models with a medium host density assumption (0.002 hosts per m^3), a density that was more consistent with what we observed in the field. However, again, this was likely an underestimate. We found that leopard frogs had a 10%, 2%, and 0% chance of maintaining *Bd* for 10 or more years when there was a seasonal maximum of 22 post-metamorphic frogs in area of $11,000 \text{ m}^3$, for Louisiana, Tennessee, and Pennsylvania, respectively.

We hypothesized that differences in seasonal minimums in *Bd* prevalence could be a more important driver of long-term *Bd* persistence than seasonal R_0 (given seasonal $R_0 > 1$). To test this hypothesis, we used our model to artificially increase *Bd* shedding rates on leopard frogs in Pennsylvania such that seasonal R_0 increased from 1.35 to 20 (where 20 is simply a biologically “large” value for R_0), but minimum *Bd* prevalence was only slightly altered (from 0.06% to 0.08%). We found that increasing seasonal R_0 from 1.35 to 20 had no discernible effect on long-term *Bd* persistence in Pennsylvania: across all leopard frog population sizes we examined, *Bd* could still never persist for >10 years on only post-metamorphic leopard frogs (Figure 4). Note, however, that differences in CCS between Tennessee and Louisiana, despite similar model-predicted minimum prevalence (9.2% and 9%), illustrates that characteristics of prevalence cycles more generally, such as time spent below a certain prevalence, also affect long-term pathogen persistence.

DISCUSSION

Seasonality is a pervasive component of wildlife disease systems but, for many systems, we still have a limited understanding of causes and consequences of seasonal

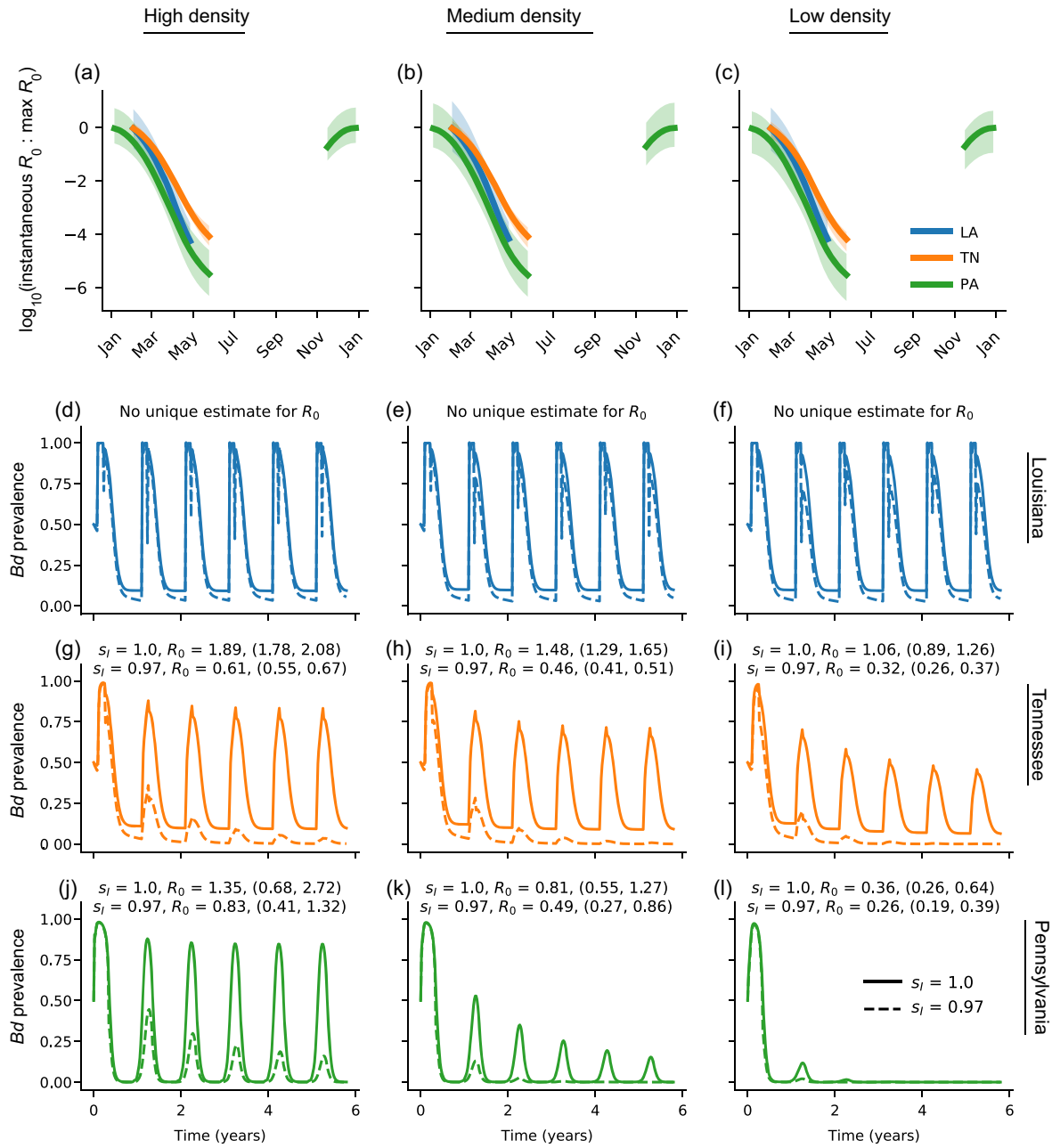


FIGURE 3 (a–c) Instantaneous R_0 across the year for leopard frogs at three different locations, as predicted by the “Baseline + temperature-dependent Bd growth” model. The values shown are the \log_{10} ratios of instantaneous R_0 at a given time compared to the maximum instantaneous R_0 within a year. Thus, higher values indicate when instantaneous R_0 is higher within the season. (a) Gives the estimated instantaneous R_0 ratios for models under a high host density assumption (~ 0.14 per m^3), (b) under a medium host density assumption (~ 0.002 per m^3), and (c) under a low host density assumption (~ 0.0003 per m^3). The colored lines give the median model predictions and the shaded region gives the 95% credible interval around the instantaneous R_0 ratios. For these predictions, temperature was modeled as a periodic function, based on observed temperatures at each location. The gaps in the colored lines indicate where post-metamorphic frogs are not in the water and transmission (and thus instantaneous R_0) is 0. (d–l) The predicted dynamics of *Batrachochytrium dendrobatidis* (Bd) prevalence given the “Baseline + temperature-dependent Bd growth” model for Tennessee (TN) and Pennsylvania (PA) and the “Baseline + temperature-dependent Bd growth and susceptibility” model for Louisiana (LA) under different host densities. Host survival given infection s_i was varied from 1 (solid lines) to 0.97 (dashed lines). Temperature was modeled as a periodic function as in (a–c) seasonal R_0 (shown as: median, [upper quartile, lower quartile]) was calculated for each combination of location, density, and survival given infection, drawing from the posterior distributions of the estimated parameters for the best-fit model. Under the “Baseline + temperature-dependent Bd growth and susceptibility” model in Louisiana, seasonal R_0 was not uniquely identifiable because the effect of temperature on transmission was not uniquely identifiable (but was negative; Appendix S3).

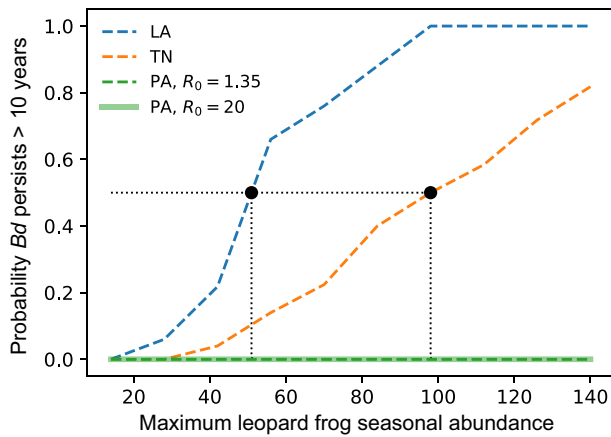


FIGURE 4 The probability of *Batrachochytrium dendrobatidis* (*Bd*) persisting for 10 years or more on only post-metamorphic leopard frogs as a function of the maximum abundance of post-metamorphic leopard frogs over the course of the year in a closed area comprising terrestrial and aquatic habitat. The persistence curves were derived from 500 stochastic simulations of the best-fit seasonal models under a high density assumption (0.14 hosts per m^3) and no disease-induced mortality in post-metamorphic frogs ($s_f = 1$) for each location over 10 years. At the completion of each stochastic simulation, we recorded whether or not *Bd* was still present in the leopard frog population. The critical community size (CCS) was defined as the population size where the probability of *Bd* persistence was 50% over 10 years (black points and dotted lines show the CCS). The solid green line shows the results of stochastic simulations where we artificially increased seasonal R_0 from 1.35 to 20 in the Pennsylvania population, but maintained similar minimum *Bd* prevalence over the course of a year

infection dynamics. Here, we found that temporal changes in *Bd* prevalence across four geographic locations were largely described by seasonal host migrations to aquatic habitats. In contrast, seasonal terrestrial-aquatic migrations could not account for variation in infection intensity (*Bd* load). We found strong evidence across locations that *Bd* growth rate decreased with increasing temperature, driving seasonal fluctuations in *Bd* load. Using these results, we then asked whether the predicted seasonal *Bd* dynamics allowed for post-metamorphic leopard frogs to act as maintenance species for *Bd*. We found that, for realistic leopard frog population sizes, demographic stochasticity in the host and pathogen made it unlikely for *Bd* to persist through seasonal troughs in prevalence, despite deterministic predictions to the contrary. Our results highlight a critical disconnect between deterministic and stochastic definitions of maintenance species in seasonal environments and the need of alternative reservoirs for long-term *Bd* persistence in these seasonal amphibian communities. In other words, if leopard frogs were the only host for the pathogen in a wetland setting, *Bd* would likely disappear within 10 years.

The mechanisms of seasonal infection dynamics

Seasonality in transmission can be separated into processes that affect contact rates between a host and pathogen and those that affect the probability of infection given contact (susceptibility). For leopard frogs, contact rates between amphibians and *Bd* are affected by seasonal migrations of leopard frogs to and from the aquatic environment for breeding and, in some locations, brumation. Moreover, constitutive defenses of leopard frogs that have been strongly linked to the probability of infection given contact, such as antimicrobial peptides (AMPs) and the skin microbiome (Holden et al., 2015; Pask et al., 2013), covary with temperature/day of year (Le Sage et al., 2021). Surprisingly, we found that seasonality in demographic processes, such as migrations to and from aquatic habitats, were generally sufficient to describe the observed seasonal patterns in *Bd* prevalence for leopard frog species. During the early spring breeding season, not only were leopard frogs in contact with the aquatic zoospore pool, but we also observed aggregations of individuals in the aquatic habitat. Our results are consistent with other wildlife systems where seasonal changes in contact rates caused by migration, denning, and seasonal aggregation drive seasonal variation in pathogen prevalence (Brown et al., 2013; Hirsch et al., 2016; Hosseini et al., 2004).

However, the drivers of seasonal disease dynamics are multifaceted (Altizer et al., 2006). In contrast to *Bd* prevalence, our models showed that, for all locations, seasonal reproduction and terrestrial-aquatic migrations were not sufficient to describe seasonal changes in *Bd* load. Instead, our models predicted a significant negative effect of temperature on *Bd* growth rate. Given that loss of infection depended on *Bd* load, the negative effect of temperature on *Bd* growth rate also contributed to seasonal patterns in *Bd* prevalence. Loss of infection probability increased in warmer temperatures as *Bd* load decreased, augmenting seasonal changes in *Bd* prevalence. Importantly, if we had ignored *Bd* load, we would have attributed observed relationships between prevalence and temperature to temperature-dependent changes in susceptibility. In contrast, we found more statistical support across three of our four locations that the relationship between prevalence and temperature was mediated by infection load, not the susceptibility component of transmission. Combined with previous work (e.g., Le Sage et al., 2021; Pask et al., 2013), our results suggest that increases in constitutive host defenses with increasing temperature reduce *Bd* growth rate on leopard frogs, leading to reduced infection intensity, which feeds back on prevalence through load-dependent loss of infection.

There were, however, notable limitations with our model. First, it is well-known that *in vitro* *Bd* growth has a non-monotonic relationship with temperature

(Piotrowski et al., 2004). Here, however, we modeled the *in vivo* temperature relationship as monotonic, which also resulted in a monotonic relationship between R_0 and temperature. While we explored including a non-monotonic effect of temperature on \log *Bd* growth rate a , this did not result in better models likely because most of our sampling occurred across temperatures where the effect on *Bd* growth rate was monotonic (e.g., Sonn et al., 2017). This limits the ability of the current model to extrapolate to changing temperature regimes. Second, we only considered mean observed water temperature over the previous week as a potential driver of transmission and within-host infection dynamics. However, it is well established that other dimensions of temperature that we did not explore, including temperature variability, mismatches between current and historic temperatures, and microclimatic temperatures within a habitat, can all affect infection dynamics (Barrile et al., 2021; Cohen et al., 2019; Raffel et al., 2013). Limitations such as model complexity, model interpretability, and parameter identifiability prevented us from including these alternative dimensions of temperature in our analysis. Thus, while we robustly identify that both seasonal host demographic and infection processes drive leopard-frog-*Bd* dynamics, other factors not considered here likely contribute to observed variability in *Bd* prevalence and infection intensity.

Pathogen maintenance potential of hosts in seasonal systems

We found strongly diverging results when we used our models to quantify the implications of seasonality on leopard frog maintenance potential of *Bd*. Despite deterministic predictions to the contrary, stochastic simulations of our models showed that it was unlikely, if not impossible, for post-metamorphic leopard frogs to maintain *Bd* for greater than 10 years on their own given realistic population sizes. Thus, even under ideal conditions of no disease-induced mortality, it seems unlikely that post-metamorphic leopard frogs can maintain *Bd* without contributions from other reservoirs of infection. While we did not attempt to identify what additional species could be contributing to *Bd* persistence in these three locations, the modeling framework we develop here can be extended to answer this question by simultaneously fitting *Bd* prevalence and infection data from multiple amphibian species in the community.

The mismatch between deterministic persistence predicted by seasonal R_0 and long-term stochastic persistence predicted by critical community size highlights two key limitations for using seasonal R_0 in a management

context. First, in seasonal host-pathogen systems, species with high seasonal R_0 but larger seasonal fluctuations in pathogen prevalence might be much less likely to be maintenance species for a pathogen than species with lower values of seasonal R_0 and smaller seasonal fluctuations in prevalence. The reason for this is that while R_0 typically has a strong correspondence with endemic prevalence in non-seasonal disease models (Keeling & Rohani, 2008), seasonality can break this correspondence such that systems with high seasonal R_0 can still have low pathogen prevalence at certain times of the year. This is a similar phenomenon to epidemic fadeout (Keeling & Rohani, 2008). Here, seasonal changes in host and pathogen vital rates, rather than the depletion of susceptible hosts, lead to troughs in pathogen prevalence and stochastic pathogen extirpation.

The second limitation of seasonal R_0 is that it likely provides an overly aggressive benchmark for disease eradication. While the conventional (and mathematically verified) wisdom is that management should aim to reduce seasonal $R_0 < 1$ for eradication of a seasonal pathogen (Bozzuto & Canessa, 2019), this might be too stringent of a criterion in some seasonal host-pathogen systems. In fact, our results suggest that if the main driver of long-term pathogen persistence is minimal seasonal prevalence, then management strategies that further reduce minimal seasonal prevalence or population abundance during this time could achieve pathogen eradication with less impact on the host population than attempting to reduce seasonal R_0 below 1. Management strategies could include ensuring habitat connectivity for dispersal away from ponds to reduce host density or increasing the availability of thermal habitats conducive to loss of infection. The generality of this result and its applicability to disease management in threatened species deserves further attention.

ACKNOWLEDGMENTS

We would like to thank the following technicians for their contributions to this work: Zoe Au, Jeff Bednark, Paradise Blackwood, Robert Campion, Lauren Chronister, Jordan Coscia, Aimee Danley, Zach Davis, Stephi Dickinson, Chip Dougherty, Nina Dunnell, Bobby Fletcher, Kaitlyn Forrest, Louis Gibson, Ben Glennon, Tali Hammond, Conor Harrington, Ally Hartman, Marcus Hough, Brady Inman, Jennifer Kassimer, Stephanie Kubik, Jessica Keeney, Kendall Kohler, Mitch Le Sage, Ryan Marsden, Cristina McCarthy, Haley McClary, Brian Miller, Maegan Murphy, Sadie Parker, Aubrey Pelletier, Natalie Popielski, Phoebe Reuben, Ayla Ross, Natalie Schroth, Samantha Shablin, Samantha Skerlec, Trina Wantman, Emily Wojtyna, Lydia Zimmerman, and Jakub Zegar. We would also like to thank the following

personnel at Fort Polk, Louisiana Division of Wildlife and Fisheries, Pymatuning Laboratory of Ecology, and private landowners for their support: Sarah Pearce, Abigail Arfman, Gregory (Kyler) McKee, Lynn Bennett, Marianne and David Solomon, Allen Solomon (1926–2020), the Solomon family, the Red River Ranch, Chris Davis, and Jessica Barabas. Protocols and permits were as follows: Louisiana (LA), U. Pitt. IACUC Protocol #1602771 and LA Department of Wildlife and Fisheries Scientific Research and Collecting Permits LNHP-17-029, LNHP-18-005, WDP-19-010; Pennsylvania (PA), U. Pitt. IACUC Protocol #1602771 and collection permits from the PA Fish and Boat Commission; Tennessee (TN), Vanderbilt IACUC #M1600250-0 and TN Wildlife Resource Agency Scientific Collection Permit #1546; Vermont (VT), UMass IACUC #2014003 and VT Fish and Wildlife Department Permit SR-2016-17. Funding was provided by the U.S. Department of Defense SERDP contract RC-2638. Photographs were used with permission from M. Ohmer and B. LaBumbard.

CONFLICT OF INTEREST


The authors declare no conflict of interest.


DATA AVAILABILITY STATEMENT

The code and data necessary to reproduce the analyses are available at <https://doi.org/10.5281/zenodo.6407088> (Wilber et al., 2022).

ORCID

Mark Q. Wilber  <https://orcid.org/0000-0002-8274-8025>

Laura A. Brannelly  <https://orcid.org/0000-0003-2975-9494>

Emily H. Le Sage  <https://orcid.org/0000-0002-2815-6651>

Corinne L. Richards-Zawacki  <https://orcid.org/0000-0002-4212-041X>

Jamie Voyles  <https://orcid.org/0000-0002-0073-5790>

REFERENCES

- Almberg, E. S., P. C. Cross, and D. W. Smith. 2010. "Persistence of Canine Distemper Virus in the Greater Yellowstone Ecosystem's Carnivore Community." *Ecological Applications* 20: 2058–74.
- Altizer, S., A. Dobson, P. Hosseini, P. Hudson, M. Pascual, and P. Rohani. 2006. "Seasonality and the Dynamics of Infectious Diseases." *Ecology Letters* 9: 467–84.
- AmphibiaWeb. 2021. "AmphibiaWeb." <https://amphibiaweb.org>.
- Bacaër, N., and E. H. Ait Dads. 2012. "On the Biological Interpretation of a Definition for the Parameter R_0 in Periodic Population Models." *Journal of Mathematical Biology* 65: 601–21.
- Barrile, G. M., A. D. Chalfoun, and A. W. Walters. 2021. "Infection Status as the Basis for Habitat Choices in a Wild Amphibian." *The American Naturalist* 197: 128–37.
- Bartlett, M. S. 1960. "The Critical Community Size for Measles in the United States." *Journal of the Royal Statistical Society. Series A* 123: 37–44.
- Bozzuto, C., and S. Canessa. 2019. "Impact of Seasonal Cycles on Host-Pathogen Dynamics and Disease Mitigation for *Batrachochytrium salamandrivorans*." *Global Ecology and Conservation* 17: e00551.
- Brannelly, L. A., R. J. Webb, D. A. Hunter, N. Clemann, K. Howard, L. F. Skerratt, L. Berger, and B. C. Scheele. 2018. "Non-declining Amphibians Can Be Important Reservoir Hosts for Amphibian Chytrid Fungus." *Animal Conservation* 21: 91–101.
- Briggs, C. J., R. A. Knapp, and V. T. Vredenburg. 2010. "Enzootic and Epizootic Dynamics of the Chytrid Fungal Pathogen of Amphibians." *Proceedings of the National Academy of Sciences USA* 107: 9695–700.
- Briggs, C. J., V. T. Vredenburg, R. A. Knapp, and L. J. Rachowicz. 2005. "Investigating the Population-Level Effects of Chytridiomycosis: An Emerging Infectious Disease of Amphibians." *Ecology* 86: 3149–59.
- Brown, V. L., J. M. Drake, D. E. Stallknecht, J. D. Brown, and K. Pedersen. 2013. "Dissecting a Wildlife Disease Hotspot: The Impact of Multiple Host Species, Environmental Transmission and Seasonality in Migration, Breeding and Mortality." *Journal of the Royal Society, Interface* 10: 20120804.
- Cayuela, H., A. Valenzuela-Sanchez, L. Teulier, Í. Martínez-Solano, J.-P. Léna, J. Merilä, E. Muths, et al. 2020. "Determinants and Consequences of Dispersal in Vertebrates with Complex Life Cycles: A Review of Pond-Breeding Amphibians." *The Quarterly Review of Biology* 45: 1–36.
- Chikerema, S. M., D. M. Pfukenyi, G. Matope, and E. Bhebhe. 2012. "Temporal and Spatial Distribution of Cattle Anthrax Outbreaks in Zimbabwe between 1967 and 2006." *Tropical Animal Health and Production* 44: 63–70.
- Clare, F. C., J. B. Halder, O. Daniel, J. Bielby, M. A. Semenov, T. Jombart, A. Loyau, et al. 2016. "Climate Forcing of an Emerging Pathogenic Fungus across a Montane Multi-Host Community." *Philosophical Transactions of the Royal Society of London B: Biological Sciences* 371: 20150454.
- Cohen, J. M., T. A. McMahon, C. Ramsay, E. A. Roznik, E. L. Sauer, S. Bessler, D. J. Civitello, et al. 2019. "Impacts of Thermal Mismatches on Chytrid Fungus *Batrachochytrium dendrobatidis* Prevalence Are Moderated by Life Stage, Body Size, Elevation and Latitude." *Ecology Letters* 22: 817–25.
- Cunjak, R. A. 1986. "Winter Habitat of Northern Leopard Frogs, *Rana pipiens*, in a Southern Ontario Stream." *Canadian Journal of Zoology* 64: 255–7.
- DiRenzo, G. V., P. F. Langhammer, K. R. Zamudio, and K. R. Lips. 2014. "Fungal Infection Intensity and Zoospore Output of *Atelopus zeteki*, a Potential Acute Chytrid Supershedder." *PLoS One* 9: e93356.
- Easterling, M. R., S. P. Ellner, and P. M. Dixon. 2000. "Size-Specific Sensitivity: Applying a New Structured Population Model." *Ecology* 81: 694–708.
- Ellner, S. P., D. Z. Childs, and M. Rees. 2016. *Data-Driven Modelling of Structured Populations*. New York, NY: Springer International Publishing.
- Finkelman, B. S., C. Viboud, K. Koelle, M. J. Ferrari, N. Bharti, and B. T. Grenfell. 2007. "Global Patterns in Seasonal Activity of

- Influenza A/H3N2, A/H1N1, and B from 1997 to 2005: Viral Coexistence and Latitudinal Gradients." *PLoS One* 2: e1296.
- Gelman, A., J. B. Carlin, H. S. Stern, D. B. Dunson, A. Vehtari, and D. B. Rubin. 2014. *Bayesian Data Analysis*. Boca Raton, FL: Taylor & Francis Group, LLC.
- González, E. J., C. Martorell, and B. M. Bolker. 2016. "Inverse Estimation of Integral Projection Model Parameters Using Time Series of Population-Level Data." *Methods in Ecology and Evolution* 7: 147–56.
- Greenspan, S. E., D. S. Bower, R. J. Webb, L. Berger, D. Rudd, L. Schwarzkopf, and R. A. Alford. 2017. "White Blood Cell Profiles in Amphibians Help to Explain Disease Susceptibility Following Temperature Shifts." *Developmental and Comparative Immunology* 77: 280–6.
- Haydon, D. T., S. Cleaveland, L. H. Taylor, and M. K. Laurenson. 2002. "Identifying Reservoirs of Infection: A Conceptual and Practical Challenge." *Emerging Infectious Diseases* 8: 1468–73.
- Hirsch, B. T., J. J. H. Reynolds, S. D. Gehrt, and M. E. Craft. 2016. "Which Mechanisms Drive Seasonal Rabies Outbreaks in Raccoons? A Test Using Dynamic Social Network Models." *Journal of Applied Ecology* 53: 804–13.
- Holden, W. M., S. M. Hanlon, D. C. Woodhams, T. M. Chappell, H. L. Wells, S. M. Glisson, V. J. McKenzie, R. Knight, M. J. Parris, and L. A. Rollins-Smith. 2015. "Skin Bacteria Provide Early Protection for Newly Metamorphosed Southern Leopard Frogs (*Rana sphenocephala*) against the Frog-Killing Fungus, *Batrachochytrium dendrobatidis*." *Biological Conservation* 187: 91–102.
- Hosseini, P. R., A. A. Dhondt, and A. Dobson. 2004. "Seasonality and Wildlife Disease: How Seasonal Birth, Aggregation and Variation in Immunity Affect the Dynamics of *Mycoplasma gallisepticum* in House Finches." *Proceedings of the Royal Society B* 271: 2569–77.
- Hyatt, A. D., D. G. Boyle, V. Olsen, D. B. Boyle, L. Berger, D. Obendorf, A. Dalton, et al. 2007. "Diagnostic Assays and Sampling Protocols for the Detection of *Batrachochytrium dendrobatidis*." *Diseases of Aquatic Organisms* 73: 175–92.
- Keeling, M., and P. Rohani. 2008. *Modeling Infectious Diseases in Humans and Animals*. Princeton, NJ: Princeton University Press.
- Kilpatrick, A. M., C. J. Briggs, and P. Daszak. 2010. "The Ecology and Impact of Chytridiomycosis: An Emerging Disease of Amphibians." *Trends in Ecology and Evolution* 25: 109–18.
- Le Sage, E. H., B. C. LaBumbard, L. K. Reinert, B. T. Miller, C. L. Richards-Zawacki, D. C. Woodhams, and L. A. Rollins-Smith. 2021. "Preparatory Immunity: Seasonality of Mucosal Skin Defences and *Batrachochytrium* Infections in Southern Leopard Frogs." *Journal of Animal Ecology* 90: 542–54.
- London, W. P., and J. A. Yorke. 1973. "Recurrent Outbreaks of Measles, Chickenpox and Mumps: I. Seasonal Variation in Contact Rates." *American Journal of Epidemiology* 98: 453–68.
- Martinez, M. E. 2018. "The Calendar of Epidemics: Seasonal Cycles of Infectious Diseases." *PLoS Pathogens* 14: e1007327.
- Merrell, D. J. 1970. "Migration and Gene Dispersal in *Rana pipiens*." *American Zoologist* 10: 47–52.
- Metcalfe, C. J. E., A. L. Graham, M. Martinez-Bakker, and D. Z. Childs. 2015. "Opportunities and Challenges of Integral Projection Models for Modelling Host–Parasite Dynamics." *Journal of Animal Ecology* 85: 343–55.
- Mordecai, E., J. Cohen, M. Evans, P. Gudapati, L. Johnson, C. Lippi, K. Miazgowiec, et al. 2017. "Detecting the Impact of Temperature on Transmission of Zika, Dengue and Chikungunya Using Mechanistic Models." *PLoS Neglected Tropical Diseases* 11: e0005568.
- Palmer, M. V. 2013. "Mycobacterium bovis: Characteristics of Wildlife Reservoir Hosts." *Transboundary and Emerging Diseases* 60: 1–13.
- Pask, J. D., T. L. Cary, and L. A. Rollins-Smith. 2013. "Skin Peptides Protect Juvenile Leopard Frogs (*Rana pipiens*) against Chytridiomycosis." *Journal of Experimental Biology* 216: 2908–16.
- Peel, A. J., J. R. Pulliam, A. D. Luis, R. K. Plowright, T. J. O'Shea, D. T. Hayman, J. L. Wood, C. T. Webb, and O. Restif. 2014. "The Effect of Seasonal Birth Pulses on Pathogen Persistence in Wild Mammal Populations." *Proceedings of the Royal Society B: Biological Sciences* 281: 20132962.
- Piotrowski, J. S., S. L. Annis, and J. E. Longcore. 2004. "Physiology of *Batrachochytrium dendrobatidis*, a Chytrid Pathogen of Amphibians." *Mycologia* 96: 9–15.
- Raffel, T. R., J. R. Rohr, J. M. Kiesecker, and P. J. Hudson. 2006. "Negative Effects of Changing Temperature on Amphibian Immunity under Field Conditions." *Functional Ecology* 20: 819–28.
- Raffel, T. R., J. M. Romansic, N. T. Halstead, T. A. McMahon, M. D. Venesky, and J. R. Rohr. 2013. "Disease and Thermal Acclimation in a more Variable and Unpredictable Climate." *Nature Climate Change* 3: 146–51.
- Rebelo, C., A. Margheri, and N. Bacaër. 2012. "Persistence in Seasonally Forced Epidemiological Models." *Journal of Mathematical Biology* 64: 933–49.
- Reeder, N. M. M., A. P. Pessier, and V. T. Vredenburg. 2012. "A Reservoir Species for the Emerging Amphibian Pathogen *Batrachochytrium dendrobatidis* Thrives in a Landscape Decimated by Disease." *PLoS One* 7: e33567.
- Roberts, M. G., and J. A. Heesterbeek. 2020. "Characterizing Reservoirs of Infection and the Maintenance of Pathogens in Ecosystems." *Journal of the Royal Society, Interface* 17: 20190540.
- Sonn, J. M., S. Berman, and C. L. Richards-Zawacki. 2017. "The Influence of Temperature on Chytridiomycosis *In Vivo*." *EcoHealth* 14: 762–70.
- Sonn, J. M., R. M. Utz, and C. L. Richards-Zawacki. 2019. "Effects of Latitudinal, Seasonal, and Daily Temperature Variations on Chytrid Fungal Infections in a North American Frog." *Ecosphere* 10: e02892.
- VanderWaal, K., M. Gilbertson, S. Okanga, B. F. Allan, and M. E. Craft. 2017. "Seasonality and Pathogen Transmission in Pastoral Cattle Contact Networks." *Royal Society Open Science* 4: 170808.
- Viana, M., R. Mancy, R. Biek, S. Cleaveland, P. C. Cross, J. O. Lloyd-Smith, and D. T. Haydon. 2014. "Assembling Evidence for Identifying Reservoirs of Infection." *Trends in Ecology and Evolution* 29: 270–9.
- Wilber, M. Q., K. E. Langwig, A. M. Kilpatrick, H. I. McCallum, and C. J. Briggs. 2016. "Integral Projection Models for Host–Parasite Systems with an Application to Amphibian Chytrid Fungus." *Methods in Ecology and Evolution* 7: 1182–94.
- Wilber, M. Q., M. E. B. Ohmer, K. A. Altman, L. A. Brannelly, B. C. LaBumbard, E. H. Le Sage, N. B. McDonnell, et al. 2022.

“mqwilber/bd_seasonality: Code for Amphibian-Bd Seasonality Analysis.” Zenodo, Dataset. <https://doi.org/10.5281/zenodo.6407088>.

- Wilber, M. Q., F. Pfab, M. E. Ohmer, and C. J. Briggs. 2021. “Integrating Infection Intensity Into Within- and between-Host Pathogen Dynamics: Implications for Invasion and Virulence Evolution.” *The American Naturalist* 198: 661–77.
- Woodhams, D. C., and R. A. Alford. 2005. “Ecology of Chytridiomycosis in Rainforest Stream Frog Assemblages of Tropical Queensland.” *Conservation Biology* 19: 1449–59.
- Woodhams, D. C., R. A. Alford, C. J. Briggs, M. Johnson, and L. A. Rollins-Smith. 2008. “Life-History Trade-Offs Influence Disease in Changing Climates: Strategies of an Amphibian Pathogen.” *Ecology* 89: 1627–39.

SUPPORTING INFORMATION

Additional supporting information may be found in the online version of the article at the publisher’s website.

How to cite this article: Wilber, Mark Q., Michel E. B. Ohmer, Karie A. Altman, Laura A. Brannelly, Brandon C. LaBumbard, Emily H. Le Sage, Nina B. McDonnell, et al. 2022. “Once a Reservoir, Always a Reservoir? Seasonality Affects the Pathogen Maintenance Potential of Amphibian Hosts.” *Ecology* 103(9): e3759. <https://doi.org/10.1002/ecy.3759>